academicJournals

Vol. 8(19), pp. 767-777, 18 May, 2013
DOI 10.5897/SRE2013.5354
ISSN 1992-2248 © 2013 Academic Journals
http://www.academicjournals.org/SRE

Scientific Research and Essays

Full Length Research Paper

Computational simulation of frequency inverter ramps applied to an electric vehicle

Francisco Jose Grandinetti[1,2],*, Luiz Octavio Mattos dos Reis[1], Wendell de Queiroz Lamas[1,3], Paulo Antonio dos Santos[1] and Denis Fernando Ramos[1]

[1]Department of Mechanical Engineering, University of Taubate, Taubate, SP, Brazil.
[2]Department of Mechanics, Faculty of Engineering at Guaratingueta, Sao Paulo State University, Guaratingueta, SP, Brazil.
[3]Department of Basic and Environmental Sciences, Engineering School at Lorena, University of Sao Paulo, 05508-070, Brazil.

Accepted 7 May, 2013

This work aims to represent acceleration/deceleration ramps generator and a voltage/frequency control through a SCICOS block diagram for evaluation of values commonly used with electric vehicles. It was opted for the representation of functional block diagrams for implementing the models, and was adopted the free software SCILAB/SCICOS to design and to simulate the representations proposed. Also measurements from electric vehicle coupled to frequency inverter were done and compared to values obtained with simulations. The diagrams for the functions of acceleration/deceleration ramps and of V/f control was implemented, being fundamentals characteristics to simulate the operation of a frequency inverter for driving induction motors. Although the analysis was limited to these characteristics, in view of a variety of functions available on the inverter, the models were presented satisfactory to the representation of the basic characteristics of an inverter in the scalar configuration.

Key words: Acceleration/deceleration ramps, electric vehicle type mini-baja, voltage/frequency control.

INTRODUCTION

Majority of industrial drives use electric motors, since they are controllable and readily available. In practice, most of these drives are based on AC induction motor because these motors are rugged, reliable, and relatively inexpensive (Patil and Kurkute, 2006).

Due to robustness, reliability, low price and maintenance free (induction motors' maintenance processes are reduced and power engines less than 50 hp are disposable), induction motors (IMs) are used in most of the industrial applications. The current adjustable speed drives (ASDs) allow making the characteristics of IMs torque versus rotation similar to the DC motors ones (Thanga Raj et al., 2009).

Computer simulation of electric motor operation is particularly useful for gaining an insight into their dynamic behaviour and electro-mechanical interaction. A suitable model enables motor faults to be simulated and the change in corresponding parameters to be predicted without physical experimentation (Liang et al., 2002).

The IMs operation through frequency inverters stands out among the techniques of AC motor drives for speed control and motor torque. In this case, the supply frequency to obtain a variation of the synchronous speed is varied, beyond adjusting the values of the supply voltage based on the frequency. Thus, a speed control and efficient torque is obtained, working with a large supply motor on the market and low maintenance costs.

The frequency inverter CFW-08 manufactured by WEG

*Corresponding author. E-mail: grandi@unitau.br. Tel./Fax: 55(12)3622-4005.

(WEG, 2004) was chosen for this application, and it provides the user with options for vector control (VVC: voltage vector control) or V/f (scalar), both programmable according to the application.

In vector mode, operation is optimized for the engine in to order to obtain a better performance in terms of torque and speed regulation. The function of "auto-tuning", available for vector control, allows the automatic adjustment of inverter parameters from identification (also automatic) of the parameters of the motor connected to the inverter.

The V/f (scalar) mode is recommended for more simple applications as the drive of most pumps and fans. In these cases, it is possible to reduce losses in the motor and in the inverter using the "quadratic V/f" function, resulting in energy savings. The V/f mode is also used when more than one motor is driven by an inverter simultaneously (multi engines applications) (WEG, 2004).

The dynamics and steady-state characteristics of induction motor drive systems and frequency converters were analysed by Shinohara and Nonaka (1987), Liu et al. (1996), Hu et al. (2000), Furukawa et al. (2002), Liang et al. (2002), Singh and Al Kazzaz (2003), Andrade and Pontes (2009), and Prazenica et al. (2011).

A comprehensive coverage of state-of-the-art power electronics and AC drive technology was provided by Bose (1997) and Almeida et al. (2010).

The PWM (Pulse Width Modulation) inverter control technique to drive induction motors was studied throughout experimental results and simulations for controlling the speed of three phase induction motor by maintaining v/f ratio at constant value by Venkatesh (1994), Trovao et al. (2002), Salerno et al. (2003), and Patil and Kurkute (2006). Other control techniques were presented, such as a double fed induction generator (DFIG) by Pereira (2004), a rotor field-oriented control (RFOC) scheme by Bojoi et al. (2006) and a symmetrical three-phase matrix-reactance frequency converter (MRFC) by Korotyeyev and Fedyczak (2009).

Modelling and control approaches for problems associated to three-phase induction motor systems, including dynamic models of frequency controlled drive, were proposed and simulation results were provided and compared to current industrial ones by Appelbaum et al. (1987a), Appelbaum et al. (1987b), Patrick and Fardo (1997), Castro Neto et al. (1999), Papafotiou et al. (2004), Zhongming et al. (2008), Mastorakis et al. (2009), Razik et al. (2009), Rinkeviciene and Petrovas (2009), and Bernal et al. (2010).

The results of simulations in SIMULINK and LabVIEW for open and closed loop system were presented in works using proportional-integral (PI) control, artificial intelligence (AI) techniques such as artificial neural network (ANN), fuzzy logic, expert systems and nature inspired algorithms (NIA), genetic algorithm and differential evolution in optimization, such as Nigim (1994), Furukawa et al. (2002), Dey et al. (2009), Thanga Raj et al. (2009), Arumugam and Ramareddy (2010), and Hosek and Diblik (2011).

This work aims to represent acceleration/deceleration ramps generator and a voltage/frequency control through a SCICOS block diagram for evaluation of values commonly used with electric vehicles.

These are important characteristics in frequency inverters parameterisation, where ramps make induction motor accelerates and decelerates linearly, when V/f control does input voltage varying proportionally to stator frequency variation, providing a constant theoretical torque.

MATERIALS AND METHODS

In this context, two important characteristics to understand the operation of a frequency inverter in scalar mode will be analysed, in order to obtain models that can represent them.

The first is the generation of acceleration and deceleration ramps, to configure the motor starting and braking, while the second is the V/f control constant. These two characteristics together allow the control of speed and torque of the motor, based on the input by an operator or a supervisory system.

It was opted for the representation of functional block diagrams for implementing the models, and was adopted the free software SCILAB/SCICOS to design and to simulate the representations proposed. Also measurements from electric vehicle coupled to frequency inverter were done and compared to values obtained with simulations.

RESULTS AND DISCUSSION

The induction motor torque equation used in this study of a transmission system for an electric vehicle type mini-baja is showed in Equation (1).

$$\tau = \frac{3pp}{2\pi f} \cdot \frac{\left(V \frac{f_1}{f_2} \right)^2}{\left(r_1 + r_2' \frac{f_1}{f_2} \right)^2 + \left(X \frac{f_1}{f_2} \right)^2} \cdot r_2' \frac{f_1}{f_2} \qquad (1)$$

Where:
pp – pair of poles;
V – voltage applied to stator;
f_1 – frequency of voltage applied to motor;
f_2 – frequency of slip;
r_1 and r'_2 – resistance of stator and rotor referred to stator;
X – reactance of stator and rotor.

Model for the acceleration ramp

The speed motor variation based on starting and braking

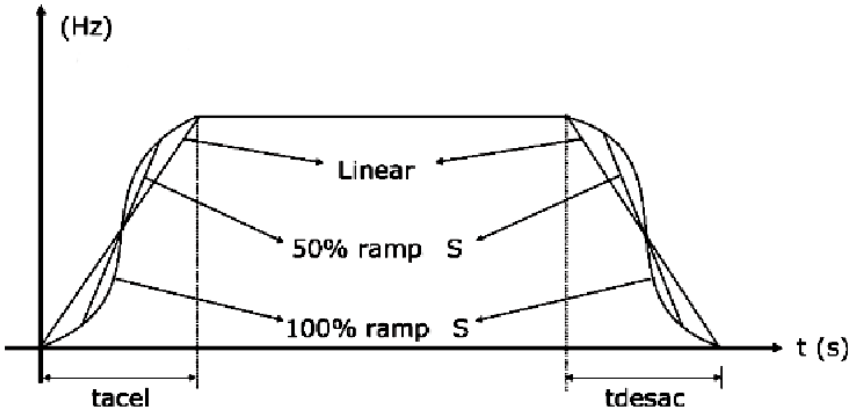

Figure 1. Acceleration, deceleration, and 'S' ramps (Mascheroni et al., 2004).

times preset by the operator are performed by acceleration and deceleration ramps. These ramps assume a linear profile, in other words, frequency (and consequently speed) increases (acceleration) or decreases (deceleration) in proportion to the time set (Fitzgerald et al., 2006). The ramp 'S' is a variation of linear ramps to produce a smooth start or stop, avoiding mechanical shocks in the system (Mascheroni et al., 2004). Figure 1 shows the two types of ramps discussed. The analysis will be restricted to linear ramps.

The representation for an acceleration ramp *f* versus *t* of an inverter can be given by a function of two sentences, as in Equation (2), where *f* is the frequency and *t* is the time.

$$f(t) = \frac{f_n}{t_a} \cdot t, \quad \text{if} \quad t < t_{ar} \; (t_{ar} - t > 0)$$

$$\text{or} \qquad (2)$$

$$f(t) = f_r, \quad \text{if} \quad t \geq t_{ar} \; (t_{ar} - t \leq 0)$$

The magnitudes characteristics are listed below:

f_n – Nominal frequency (adjustable according to the frequency of three-phase induction motor);
f_r – Reference frequency (adjustable according to operation requirements);
t_a – Nominal acceleration time;
t_{ar} – Acceleration time till the reference frequency.

The graphical representation of this expression is shown in Figure 2.

Based on the principles from Figure 2, a model will be implemented in the form of block diagrams to simulate the characteristics of the acceleration ramp in question. To the reproduction of function of two sentences, will be needed the input magnitudes f_n, t_a and f_r, which can be typed by the operator in the human-machine interface (HMI) of the inverter, for example. Figure 3 shows a block diagram proposed to exhibits the acceleration ramp, mounted from SCICOS editor of the free software SCILAB.

The nominal frequency and the acceleration time are combined to form the inclination f_n/t_a, which combined with the reference frequency generates t_{ar}. The difference $t_{ar} - t$, in the control input, has the function base comparison for the key switch in the choice of the two output options. The first is the crescent linear function, formed by multiplying the inclination by the time, selected when $t_{ar} - t > 0$, the second is the actual reference frequency, according to the condition $t_{ar} - t \leq 0$.

The simulation of the previous diagram, showed in Figure 4, results in the desired ramp profile.

It is noteworthy that, having the input f_n = 60 Hz, f_r = 30 Hz e t_a = 10 s, the acceleration time is 5 s, half of the time in the nominal frequency; it is the expected result for a linear function. The output of the diagram will be used as input in deceleration diagram to form a starting-braking set of the three-phase induction motor.

Model for the deceleration ramp

For the deceleration, beyond the known magnitudes, are still defined the nominal deceleration time (t_d), the deceleration time from f_r to 0 (t_{dr}) and the start time (t_o), since the process occurs after the acceleration and constant speed of the motor. In this case, the function of two sentences that express this characteristic is given by Equation (3).

$$f(t) = f_r - \frac{f_n}{t_d} \cdot (t - t_o), \quad \text{if} \quad t - t_o < t_{dr} \quad \text{or} \quad t_{dr} - (t - t_o) > 0 \qquad (3)$$

$$f(t) = 0, \quad \text{if} \quad t - t_o \geq t_{dr} \quad \text{or} \quad t_{dr} - (t - t_o) \leq 0$$

The graphic of this function is showed in Figure 5.

From t_o to $t_o + t_{dr}$, the ramp is a decreasing linear function with inclination $-f_n/t_a$, varying from f_r to 0,

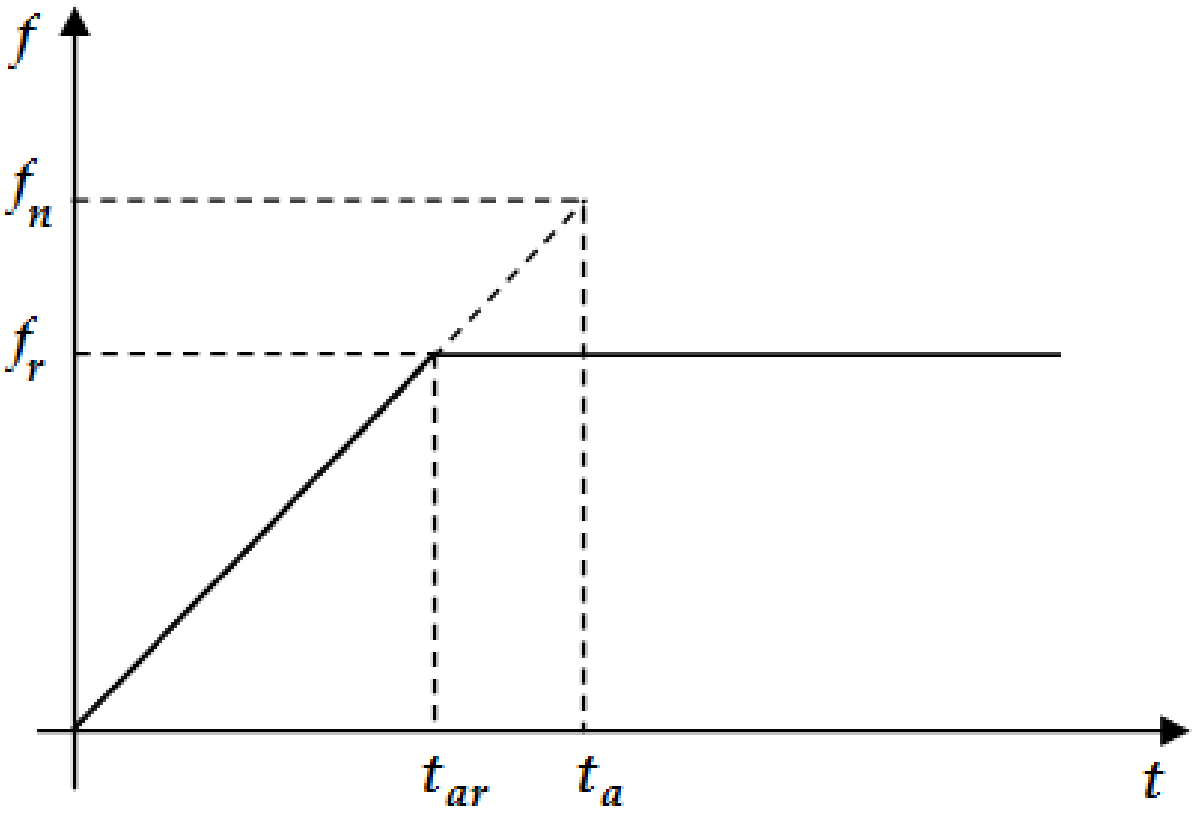

Figure 2. Acceleration ramp, with characteristics magnitudes. From 0 to t_{ar}, the ramp assumes the characteristic of a crescent linear function inclined by f_n/t_a, starting from 0 to f_r. Upon reaching the value f_r, the function becomes constant, closing the acceleration cycle. It is noteworthy that, during acceleration, the inverter operates based on the inclination f_n/t_a, in other words, to a lower frequency than f_n, the acceleration time will be lesser than t_a.

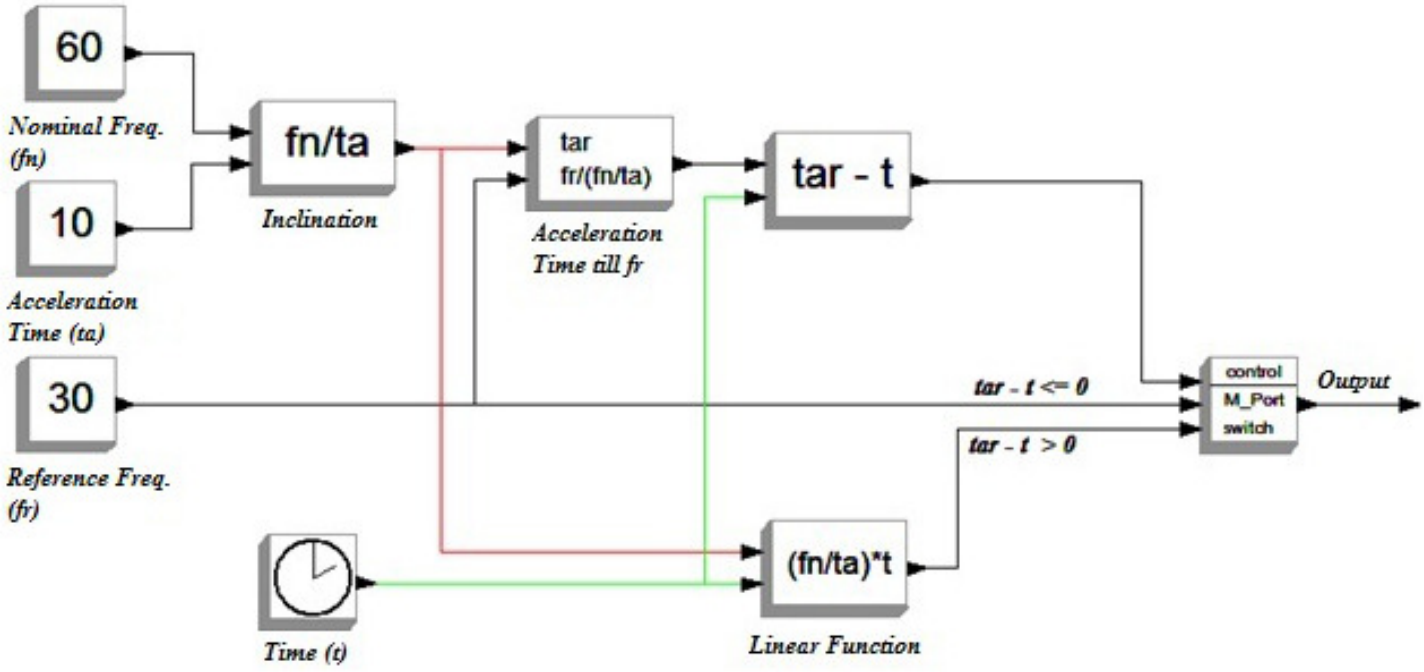

Figure 3. Block diagram for generating an acceleration ramp.

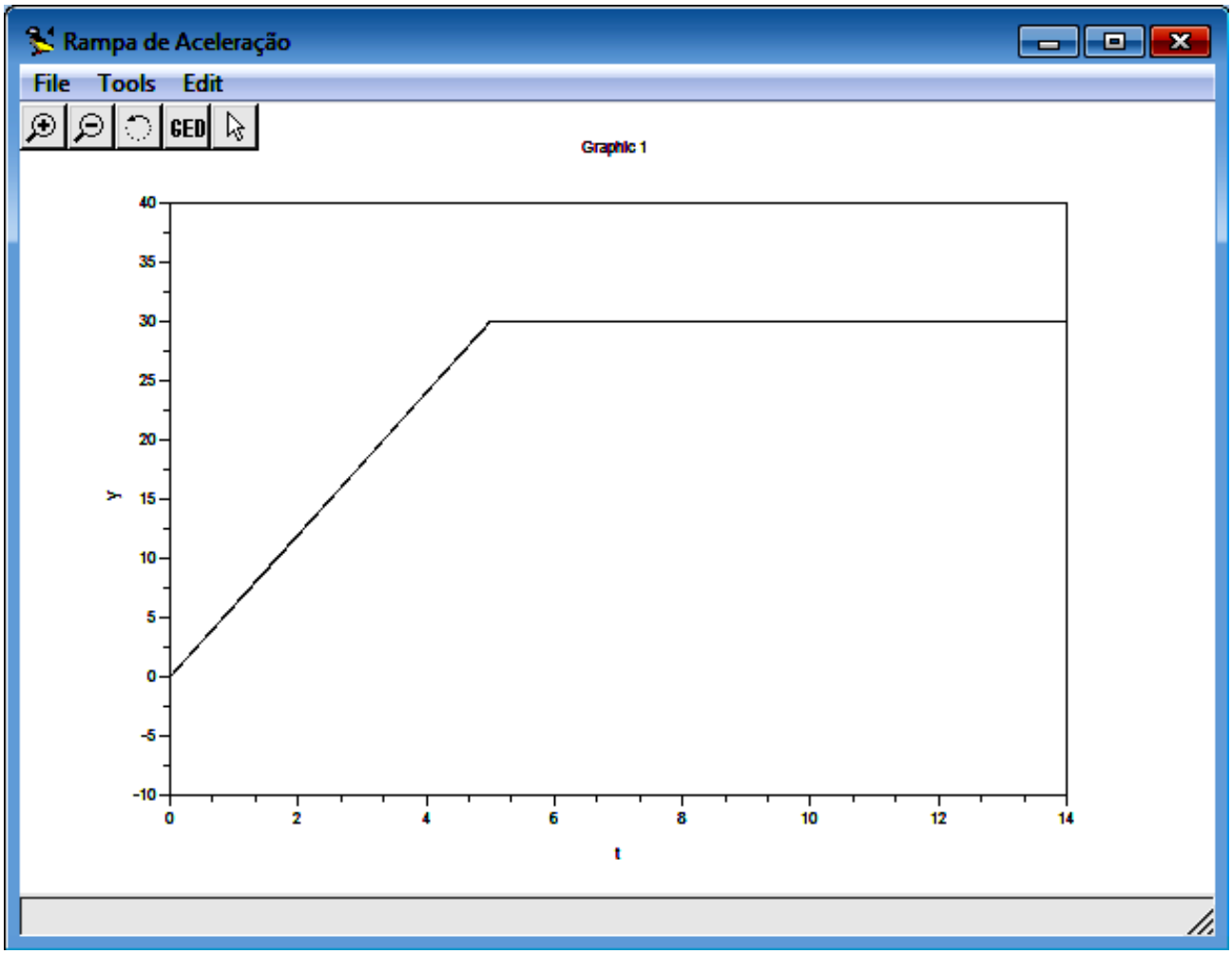

Figure 4. Acceleration ramp resulted from the simulation of the block diagram.

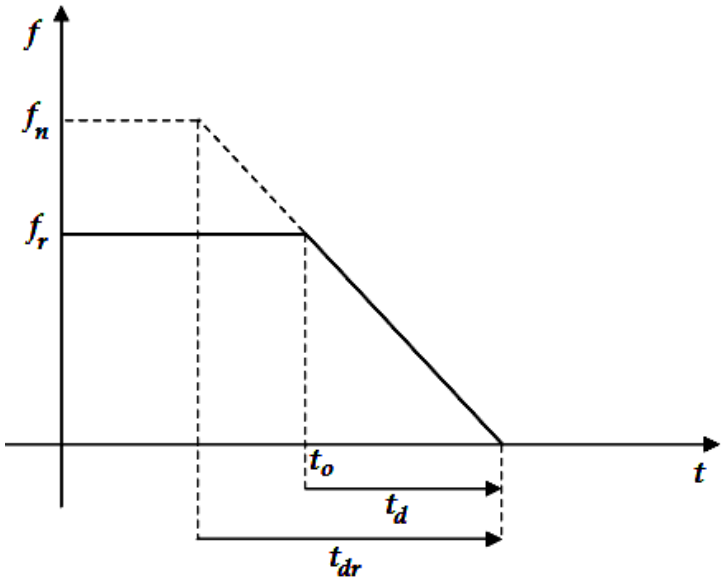

Figure 5. Deceleration ramp, from a time t_o

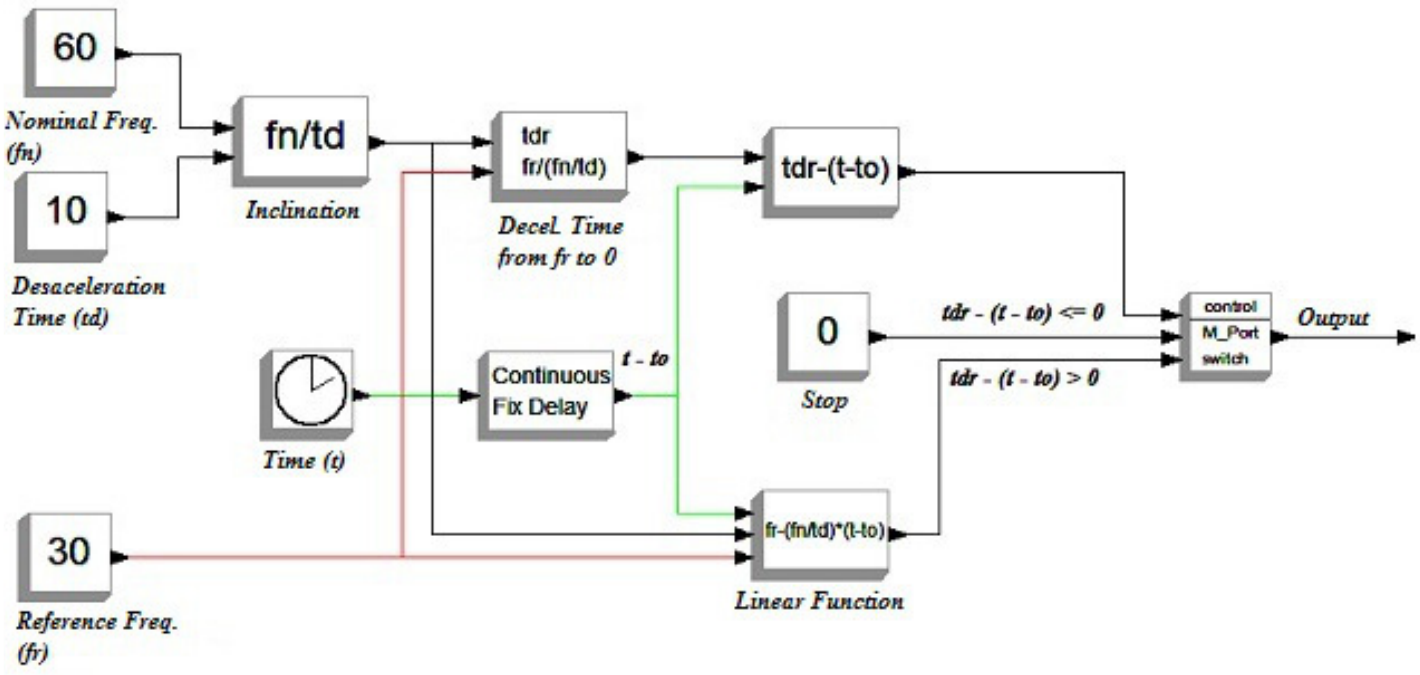

Figure 6. Block diagram for generating a deceleration ramp.

completing the deceleration phase. Since the process occurs after the acceleration cycle, the frequency enters with value f_r, dropping to 0. Just as in the acceleration, the inverter operates in the inclination $-f_n/t_a$, that is, to a lower frequency than f_n, the deceleration time will be shorter than t_d.

For the deceleration, it is proposed the block diagram in Figure 6.

As it can be observed, the control reference is made from the inclination f_n/t_d, combined with f_r to generate t_{dr}, from which it is subtracted $t - t_o$. The outputs that will be selected by the key are, in this case, the linear function while the control signal is positive, and 0 in the situation of negative or null signal. Additionally, it was inserted a time delay block (delay), since the beginning of the deceleration will occur sometime after the acceleration.

From the deceleration diagram results the desired graphic, shown in Figure 7. The reference values, in this case, were f_n = 60 Hz, f_r = 30 Hz, t_d = 10 s and the delay 10 s.

In fact, the time delay represents the moment in which the operator or supervisory system activates the stop command of the motor.

Grouping the two diagrams in cascade (Figure 8), it is obtained the configuration for generating an acceleration ramp (motor start) and a deceleration ramp (motor braking).

The resulting graphic can be observed in Figure 9, where entries were f_n = 60 Hz, f_r = 30 Hz, t_a = 10 s, t_d = 5 s and a delay of to = 10 s.

Model for the control of V/f constant

This control maintains the output voltage of the motor directly proportional to the output frequency, so that the ratio V/f will be constant during the operation of the inverter. Thus, the motor will operate with nearly constant flow, which combined with the variation of the synchronous speed by the frequency, will produce an approximately constant torque during operation (WEG, 2004).

The control V/f can be represented from a single block, which has as inputs V_n, f_n and f_r, and as output the voltage adjusted by frequency, as showed in Figure 10. The tension adjustment is done by the linear relationship with inclination V_n/f_n. It was utilized, the nominal values V_n = 220 V and f_n = 60 Hz, with f_r being an inclination ramp 60 Hz/30 s.

Practice of motor drive

The main features of an electric vehicle are economy, flexibility, and, overall, it is not a polluter, then it has drawn the attention from automotive manufacturers.

The principles of an electric motor for automotive uses are the same of the other ones, such as those used with electrical trains: a rotor (mobile part) spin over a stator (fixed part) under effect of a magnetic field generated electrically. This rotor axis transmits motion to the functional parts, in this case to the electric vehicle

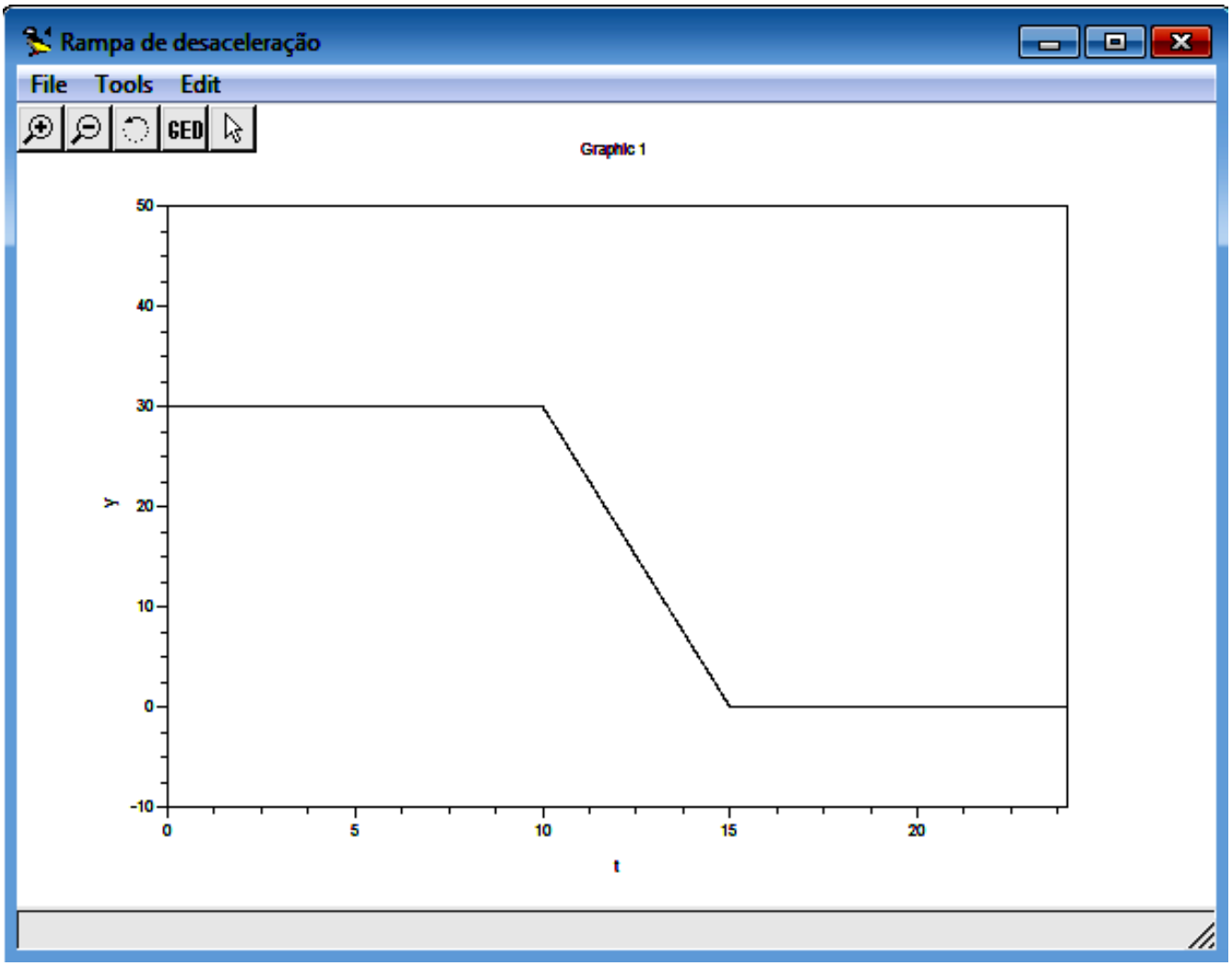

Figure 7. Acceleration ramp resulted from the simulation of the block diagram.

Table 1. Characteristics of full system.

Characteristic	Description
Load type	Rear axle of mini-baja (suspended)
Induction motor	110 V_{AC}; 60 Hz; 1.5 hp; 1,680 rpm
Frequency inverter	230 V_{AC}; 2 kW

wheels. A gearbox and a differential are placed on a "drive shaft" to adapt their speed to the wheel spokes that depend on the acceleration or deceleration (Patrick and Fardo, 1997).

There is a project called “mini-baja” at University of Taubate, where this main goal is to provide to students contact with design proceedings as a course lecture and practice. This vehicle prototype has size, weight and durability features demanded by a typical three phase induction motor of 1.5 hp (1.134 kW), which it was adapted to its transmission system. Figure 11 shows original mini-baja configuration.

The motor control was improved by a frequency inverter, which provided better efficiency and batteries use. The transmission of motor axis motion to vehicle wheels was done through a speed reducer with a transmission relation of 2.53:1, thus reducing wheels rotating and increasing their torque. Also, were adopted a yield of 0.89 and wheel radius of 24 cm. The new arrangement is showed in Figure 12.

Table 1 shows characteristics of full systems those were adjusted to these practices. Some assumptions also are used: V/f curve constant; ramp linear; torque boost of 0%; slip compensation of 0%; cut-off voltage 220 V_{AC} adjusted to 120 Hz, such 60 Hz = 110 V_{AC}; motor coupled to rear axle of mini-baja.

Table 2 relates results from practices of mini-baja with its motor connected to frequency inverter, such as showed in Figure 12.

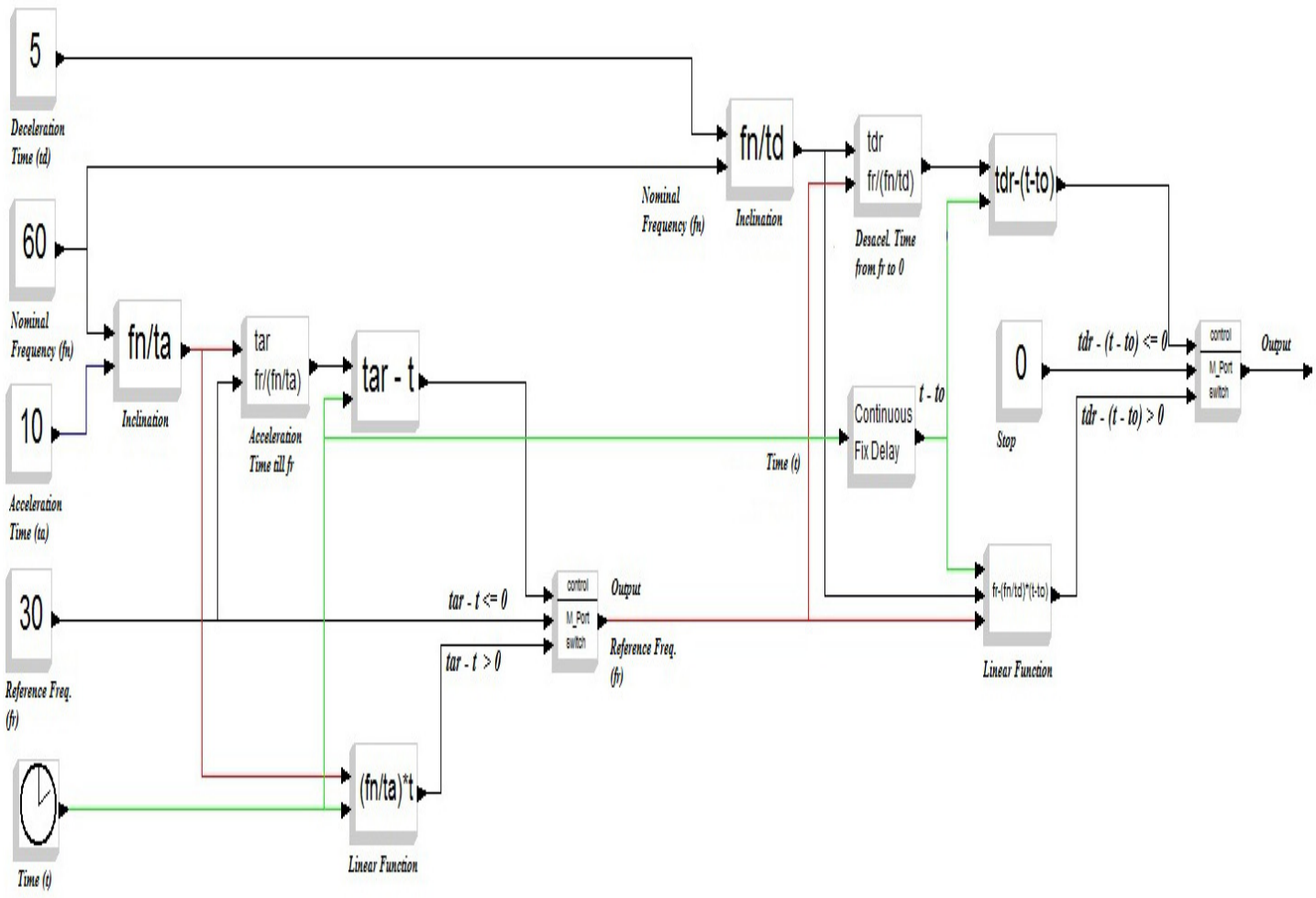

Figure 8. Model of block diagram for generating an acceleration ramp and a deceleration ramp in a single system.

Table 2. Results obtained for conditions pre-established.

Frequency adjusted in inverter (f) [Hz]	Load torque [%]	Acceleration time measured (t) [s]	Rotation measured in motor (n) [rpm]
30	35	6	891
40	35	8	1,185
50	35	10	1,488
60	35	12	1,785

Conclusions

The diagrams for the functions of acceleration/ deceleration ramps and of control V/f was implemented, being the fundamentals characteristics to simulate the operation of a frequency inverter for driving induction motors. Although the analysis was limited to these characteristics, in view of a variety of functions available on the inverter, the models present satisfactory to the representation of the basic characteristics of an inverter in the scalar configuration. Thus, a more didactic view of the equipment operation can be shown.

The results obtained with frequency inverter practices provided a validation for simulation programmed, because their values are very near. Thus, this methodology of study showed a viable way to test and develop a system based on frequency inverter for use in an electric vehicle, also optimizing its performance.

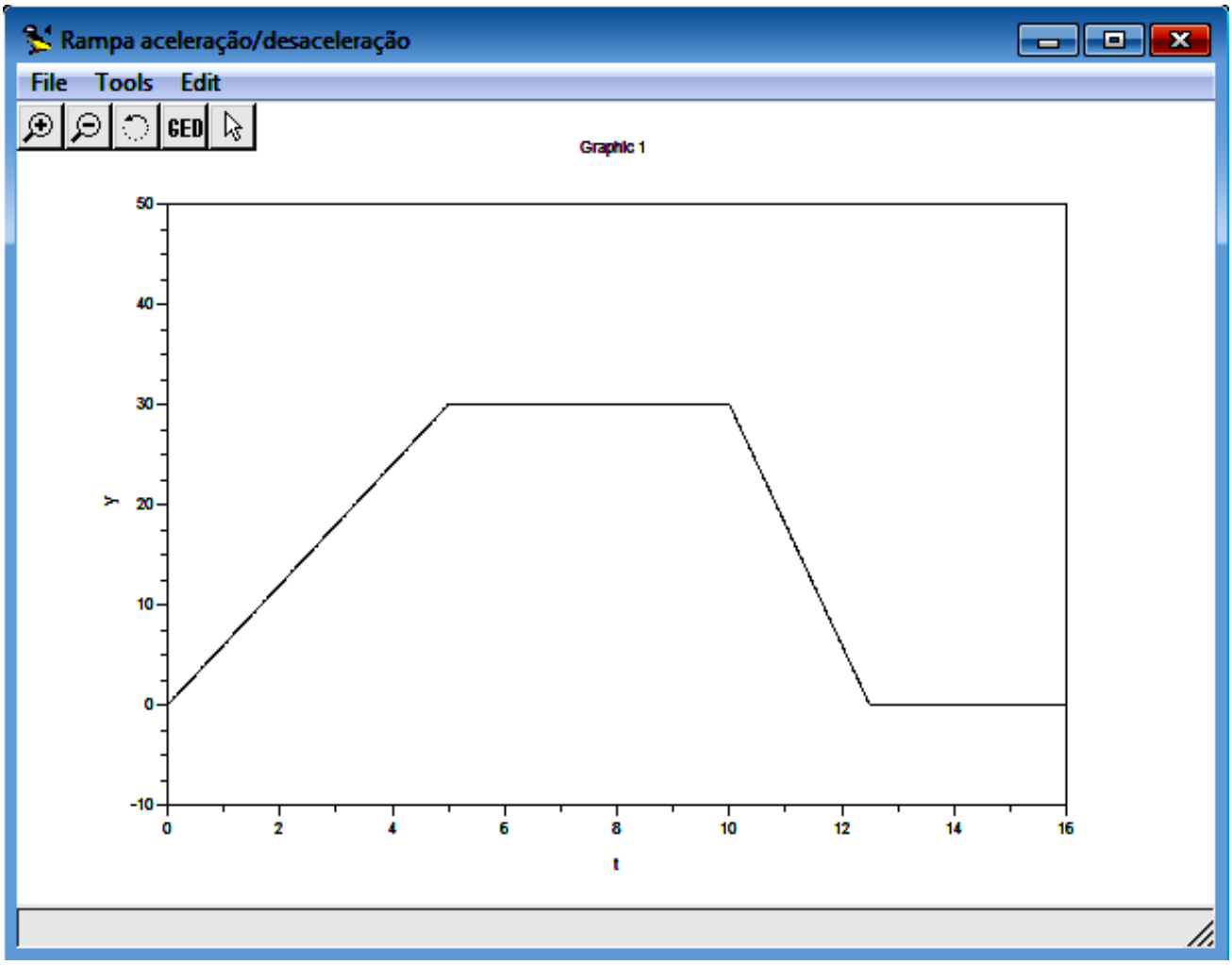

Figure 9. Acceleration and deceleration ramps generated by the unified diagram

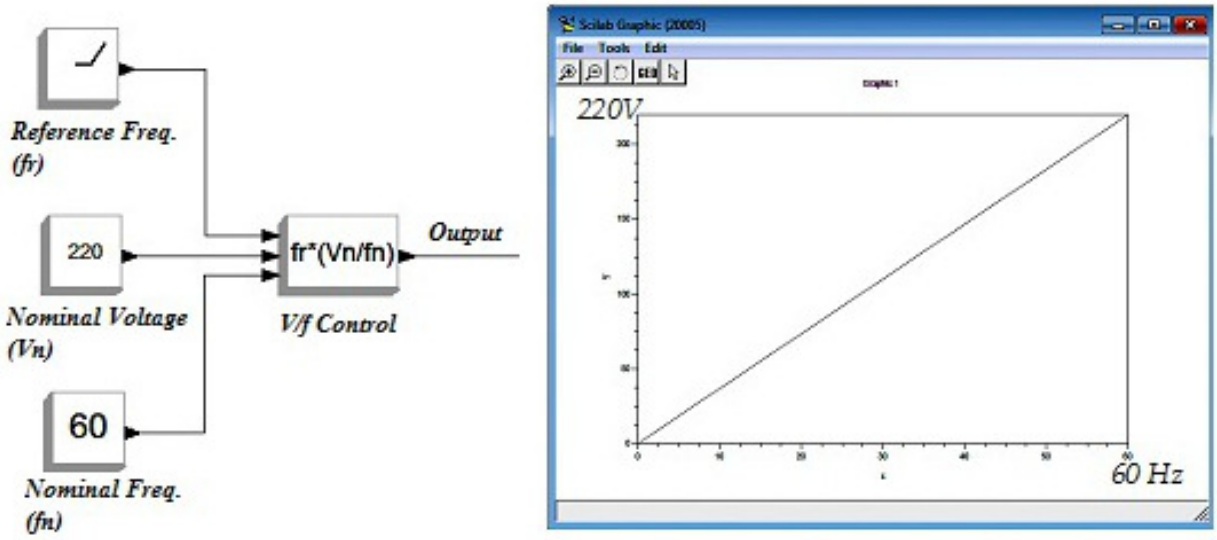

Figure 10. Basic diagram of a linear control V/f.

Figure 11. Electric vehicle type mini-baja Mini-baja has chassis single seat cage type with 1020 tubular steel frame, where length is 2 m, width is 1 m, height is 1.55 m, wheelbase is 1.70 m, and weight is around 205 kg. Its electric motor rated at 1.134 kW with maximum speed of 1,680 rpm, extruded in aluminium frame that significantly reduces its weight. Other characteristics are electronic speed controller and mechanical transmission of the drive system.

Figure 12. Electric vehicle connected to frequency inverter.

ACKNOWLEDGEMENT

Corresponding author thanks CNPq on its support through productivity scholarship on technological development and innovative extension.

REFERENCES

Almeida CVR, Oliveira A, Cerqueira JJF, Lima ACC (2010). Equipment to estimate torque in three phase induction motors by the method of slip aided by spectral analysis of stator current signal: The development and implementation. In: XVIII Congresso Brasileiro de Automatica: Proceedings of an international conference held at Bonito, MS, Brazil, pp. 4283-4288.

Andrade CTC, Pontes RST (2009). Three-phase induction motors energy efficiency standards: a case study. In: 11a. Conferencia Hispano-Lusa de Ingenieria Electrica: Proceedings of an international conference held at Zaragoza, Spain. Zaragoza: AEDIE/APDEE.

Appelbaum J, Fuchs EF, White JC (1987a). Optimization of three-phase induction motor design part I: Formulation of the optimization technique. IEEE Trans. Energ. Convers. EC-2(3):407-414.

Appelbaum J, Khan IA, Fuchs EF, White JC (1987b). Optimization of three-phase induction motor design part II: The efficiency and cost of an optimal design. IEEE Trans. Energ. Convers. EC-2(3):415-422.

Arumugam S, Ramareddy S (2010). Simulation of class E inverter based induction heater using SIMULINK. Int. J. Comp. Electr. Eng. 2(6):1081-1085.

Bernal C, Oyarbide E, Molina P, Mediano A (2010). Multi-frequency model of a single switch ZVS class E inverter. In: 2010 IEEE International Symposium on Industrial Electronics (ISIE): Proceedings of an International Conference held at Bari, Italy. pp. 939-944.

Bojoi R, Tenconi A, Griva G, Profumo F (2006). Vector control of dual-three phase induction motor drives using two current sensors. IEEE Trans. Ind. Appl. 42(5):1284-1292.

Bose BK (1997). Power electronics and variable frequency drives: Technology and applications. IEEE PRESS, New York.

Castro Neto LM, Camacho JR, Salerno CH, Alvarenga BP (1999). Analysis of a three-phase induction machine including time and space harmonic effects: The A, B, C reference frame. PES-IEEE Trans. Energ. Convers. 14(1):1-6.

Dey A, Singh B, Dwivedi B, Chandra D (2009). Vector control of three-phase induction motor using artificial intelligent technique. ARPN J. Eng. Appl. Sci. 4(4):57-67.

Fitzgerald AE, Kingsley, Jr C, Umans SD (2006). Electrical machines with introduction to power electronics. 6 ed. Bookman, Porto Alegre, RS. [in Portuguese].

Furukawa R, Yokoyama R, Koyanagi K (2002). Simulation studies on power control of doubly fed rotary frequency converter. Int. J. Electr. Pow. Energ. Sys. 24(1):1-7.

Hosek P, Diblik M (2011). Implementation of Siemens USS Protocol into LabVIEW. J. Lab. Autom. 16(5):347-354.

Hu K, Yokoyama R, Koyanagi K (2000). Modeling and dynamic simulations of doubly-fed rotary frequency converter in power systems. In: International Conference on Power System Technology: Proceedings of an International Conference held at Perth, WA, Australia, 3:1443-1448.

Korotyeyev IY, Fedyczak Z (2009). Steady and transient states modelling methods of matrix-reactance frequency converter with buck-boost topology. COMPEL: Int. J. Comp. Math. Electr. El. Eng. 28(3):626-638.

Liang B, Payne BS, Ball AD, Iwnicki SD (2002). Simulation and fault detection of three-phase induction motors. Math. Comput. Simul. 61(1):1-15.

Liu T-H, Lin C-Y, Yang J-S, Chang W-Y (1996). Modeling and performance of a static frequency converter starting a 300 MVA synchronous machine. Electr. Pow. Sys. Res. 37(1):45-53.

Mascheroni JM, Lichtblau M, Gerardi D (2004). Guide for application of frequency inverters. 2 ed. WEG Automacao, Jaragua do Sul, SC. [in

Portuguese].
Mastorakis NE, Bulucea CA, Nicola DA (2009). Modeling of three-phase induction motors in dynamic regimes according to an ecosystem pattern. In: The 13th WSEAS International Conference on Systems: Proceedings of an International Conference held at Rodos, Greece. pp. 338-345.
Nigim KA (1994). PC based single and three phase induction motor drive performance simulation. In: The 7th Mediterranean Electrotechnical Conference: Proc. Int. Conf. held at Antalya, Turkey. Porto: FEUP, 3:1255-1258.
Papafotiou G, Geyer T, Morari M (2004). Optimal direct torque control of three-phase symmetric induction motors. In: 43rd IEEE Conference on Decision and Control: Proceedings of an International Conference held at Atlantis, Paradise Island, Bahamas, pp. 1860-1865.
Patil PM, Kurkute SL (2006). Speed control of three phase induction motor using single phase supply along with active power factor correction. ACSE J. 6(3):23-32.
Patrick DR, Fardo SW (1997). Rotating Electrical Machines and Power Systems. 2 ed. Ch 11. Fairmont Press, Lilburn, GA.
Pereira MM (2004). A study of a variable speed wind turbine and its application for delivery of constant electric power. MSc thesis, Federal University of Juiz de Fora, Juiz de Fora, MG, Brazil. [in Portuguese]
Prazenica M, Dobrucky B, Sekerak P, Kalamen L (2011). Design, modelling and simulation of two-phase two-stage electronic system with orthogonal output for supplying of two-phase ASM. Mech. 9(1):56-64.
Razik H, Henao H, Carlson R (2009). An induction machine model including interbar currents for studying performances during transients and steady state. Electr. Pow. Sys. Res. 79(1):181-189.
Rinkeviciene R, Petrovas A (2009). Modelling of frequency controlled induction drive with ventilator type load. El. Electr. Eng. 6(94):69-72.
Salerno CH, Camacho JR, Oliveira-Filho AS (2003). Speed control of three-phase induction motor using microcontrollers applied to low power. In: III Seminario Nacional de Controle e Automacao: Proceedings of a National Workshop held at Salvador, Brazil. Salvador: UFBA, pp. 105-110.
Shinohara K, Nonaka S (1987). Stability improvement of a current source inverter-induction motor drive system. Autom. 23(2):161-173.
Singh GK, Al Kazzaz SAS (2003). Induction machine drive condition monitoring and diagnostic research: A survey. Electr. Pow. Sys. Res. 64(2):145-158.
Thanga Raj C, Srivastava SP, Agarwal P (2009). Energy efficient control of three-phase induction motor: A review. Int. J. Comp. Electr. Eng. 1(1):61-70.
Trovao J, Ferreira F, Francisco L, Carvalho J (2002). Comuting frequency effects of a PWM inverter in binary of a three-phase induction motor. In: Conferencia Cientifica e Tecnologica em Engenharia: Proceedings of an International Congress held at Lisboa, Portugal. Lisboa: Instituto Superior de Engenharia de Lisboa, 8 pp.
Venkatesh SC (1994). The development of a digital controller for a three-phase induction motor. MSc thesis, Massachusetts Institute of Technology, Massachusetts, USA.
WEG Automacao (2004). Frequency inverter CFW-08. User's guide version 5.2X. WEG Automacao, Jaragua do Sul, SC. [in Portuguese]
Zhongming Y, Jain PK, Sen PC (2008). Modeling of high frequency resonant inverter system in phasor domain for fast simulation and control design. In: IEEE Power Electronics Specialists Conference: Proceedings of an International Conference held at Rhodes, Greece, pp. 2090-2096.